International Journal for Housing Science and Its Applications
Publish August 6, 2025. Volume 46, Issue 3 Pages 5394-5403

https://doi.org/10.70517/ijhsa463465

Research on optimized design of heat transfer performance of air conditioner heat exchanger based on fluid dynamics simulation

Yan Hou[1,*], Yan Xiang[1] and Xin Xiao[2]
[1] School of Intelligent Construction and Environmental Engineering, Chengdu Textile College, Chengdu, Sichuan, 611731, China
[2] Minmetals Land Limited (Chengdu), Chengdu, Sichuan, 610039, China
Corresponding authors: (e-mail: houyan0712@163.com).

Abstract This paper takes the optimization of heat transfer performance of air conditioner heat exchanger as the core objective, combines with fluid dynamics simulation technology, and systematically discusses the optimization design of heat exchanger. Through the establishment of porous medium model and K-Epsilon turbulence model, ICEM CFD software is used to complete the meshing and numerical simulation. Combined with the verification of grid independence and comparison of empirical formulas, the calculation accuracy is ensured. A conventional shell-and-tube heat exchanger is taken as the research object to analyze the sensitivity of parameters such as pitch and tilt angle to Nusselt number and pressure drop, and propose an optimization scheme based on the balance between heat transfer efficiency and energy consumption. Selecting $S = 2.5mm$ and $\theta = 40°$ as the optimized structural parameters, the optimized air-conditioning heat exchanger heat transfer efficiency is increased by an average of 350W/(m2-K), the heat transfer efficiency is increased by about 10%, the energy consumption is reduced to 129kW, the footprint is reduced by about 52m, and the maintainability is increased by 26%. The four parameters of the air conditioning heat exchanger under the optimization scheme of this paper, namely, total heat transfer, latent heat, latent heat percentage and dehumidification, are all the largest, which verifies the validity of the optimized design and its applicability in engineering.

Index Terms air-conditioning heat exchanger, fluid dynamics, porous media model, K-Epsilon turbulence model, meshing

I. Introduction

In recent years, China's economy has been developing rapidly, and the construction of various infrastructures and public buildings has been in full swing, which has led to an increasing demand for various air conditioning products. On the one hand, the public requires air conditioning systems to provide a more comfortable environment, which includes maximizing the amount of fresh air introduced into the air conditioning system [1], [2]. On the other hand, the energy shortage brought about by economic growth is also a serious threat to the long-term development of the Chinese economy, and the energy consumption of infrastructure, including the energy consumption of air-conditioning systems, is a major aspect of the overall energy consumption [3]-[5]. Therefore, seeking an air conditioning system that can take into account both environmental comfort and energy consumption has become an important research topic in the HVAC industry [6], [7]. While the air conditioning heat exchanger as an important component of air conditioning, its air-side airflow distribution uniformity is one of the important factors affecting the performance [8], [9].

Fluid dynamics (CFD) simulation technology is based on the development of computer technology and numerical computation technology, the essence of which is the use of computers to solve the various conservation control partial differential equations of fluids, the application of which has been increasingly recognized in the industrial field [10]. Computational fluid dynamics technology is used to simulate and analyze the air flow in the corresponding region of the air conditioning heat exchanger, by observing the information of flow field distribution and heat exchanger surface velocity in the air conditioning unit, so as to provide a theoretical basis for the air conditioning system performance improvement [11]-[14].

In this paper, the porous medium model and turbulence model of the heat exchanger are firstly established, and the control equations and boundary conditions are clarified. Typical shell and tube heat exchanger parameters are selected as the data source to analyze the influence of geometric parameters on the flow and heat transfer

characteristics. The design optimization scheme for heat transfer performance is used to verify its practical engineering value.

II. Optimized design of heat transfer performance of air conditioner heat exchanger based on fluid dynamics

Air conditioning heat exchanger as the core component of the air conditioning system, its heat transfer efficiency and energy consumption characteristics directly affect the overall energy efficiency of the system. However, the problems of high flow resistance and uneven heat transfer in the traditional heat exchanger design have restricted its performance improvement. In recent years, optimization methods based on fluid dynamics simulation have gradually become a research hotspot due to their high efficiency and economy. In this paper, through theoretical modeling, numerical simulation and experimental verification, the optimization scheme of air-conditioning heat exchanger is systematically elaborated.

II. A.Numerical simulation methods

II. A. 1) Control equations

The foundation of CFD is based on the basic governing equations of fluid mechanics - the continuity equation, the momentum equation and the energy equation - and any flow must comply with these three basic equations of physics. Since the cross-flow fan does not need to consider temperature exchange, and can be assumed to be a two-dimensional flow field, its two-dimensional continuity equation, momentum equation expression are:

Continuity equation:

$$div(u) = 0 \tag{1}$$

Momentum equation:

$$\frac{\partial(\rho u)}{\partial t} + div(\rho uu) = div(\mu gradu) - \frac{\partial p}{\partial x} + \left[-\frac{\partial(\rho \overline{u'^2})}{\partial x} - \frac{\partial(\rho \overline{u'v'})}{\partial y} \right] + S_u \tag{2}$$

$$\frac{\partial(\rho v)}{\partial t} + div(\rho vu) = div(\mu gradv) - \frac{\partial p}{\partial y} + \left[-\frac{\partial(\rho \overline{u'v'})}{\partial x} - \frac{\partial(\rho \overline{v'^2})}{\partial y} \right] + S_v \tag{3}$$

where ρ is the fluid density, u is the velocity in the x direction, v is the velocity in the y direction, t is the time, p is the pressure, μ is the coefficient of kinetic viscosity, c_p is the specific heat capacity of the fluid, and S_u, S_v are the source terms of the equation.

Since the studied object eccentric vortex is a turbulent flow, in order to examine the effect of turbulent pulsation on the flow field in the actual flow, the time-averaging method is introduced, i.e., turbulence is considered to be a composite flow consisting of the superposition of advection and instantaneous pulsation flow. At this point, for any variable Φ, the Reynolds averaging method can be used to define the time-averaged value of the variable as:

$$\overline{\Phi} = \frac{1}{\Delta t}\int_t^{t+\Delta t} \Phi(t)dt \tag{4}$$

The "-" in the superscript represents averaging over time. The Φ' represents the pulsation value of the variable, which can be written as the sum of the average and pulsation values of the instantaneous value of the master variable, i.e.:

$$\Phi = \overline{\Phi} + \Phi' \tag{5}$$

The Reynolds time-averaged equation can be obtained by applying the Reynolds averaging method to the basic equations of fluid mechanics. Considering the actual research object of this paper, it is assumed that the fluid satisfies the following conditions:

(1) The flow is a two-dimensional problem, and the coordinate system parameter is (x, y);

(2) The fluid is an incompressible fluid with a constant density;
(3) The temperature difference of the fluid is neglected and the energy equation is ignored;
(4) Neglect the mass force effect and satisfy the Boussinesq assumption.

Then the tensor forms of the continuity and momentum equations of the fluid in the Cartesian coordinate system (x, y) are:

Continuity equation:

$$\frac{\partial(u_i)}{\partial x_i} = 0 \tag{6}$$

Momentum equation:

$$\frac{\partial(\rho u_i)}{\partial t} + \frac{\partial(\rho u_i u_j)}{\partial x_j} = -\frac{\partial p}{\partial x_i} + \frac{\partial}{\partial x_j}\left[\mu\left(\frac{\partial u_i}{\partial x_j} + \frac{\partial u_j}{\partial x_i}\right)\right] + \frac{\partial}{\partial x_j}\left(-\rho\overline{u_i' u_j'}\right) \tag{7}$$

where, $u_i, u_j (i, j = x, y)$ are the velocity components in the two coordinate directions x, y, ρ is the fluid density $\left(kg/m^3\right)$, p is the pressure (Pa), and μ is the coefficient of the fluid's dynamic viscosity $(Pa \cdot s)$. $-\rho\overline{u_i' u_j'}$ is the Reynolds stress. According to Boussinesq assumption:

$$-\rho\overline{u_i' u_j'} = -p_t \delta_{ij} + \mu_t\left(\frac{\partial u_i}{\partial x_j} + \frac{\partial u_j}{\partial x_i}\right) - \frac{2}{3}\mu_t \delta_{ij}\frac{\partial u_k}{\partial x_k} \tag{8}$$

where μ_t is the turbulent viscosity coefficient $(Pa \cdot s)$ and P_t is the pressure due to the pulsating velocity, defined as:

$$P_t = \frac{1}{3}\left(\rho\overline{u'^2} + \overline{v'^2} + \overline{w'^2}\right) = \frac{2}{3}\rho k \tag{9}$$

δ_{ij} is the Dirac function with the mathematical expression:

$$\delta_{ij} = \begin{cases} 1 & (i = j) \\ 0 & (i \neq j) \end{cases} \tag{10}$$

The turbulence model needs to be supplemented in the solution thus making the equations closed.

II. A. 2) Heat exchanger porous media modeling

There are experiments can be known that when the air flow through the heat exchanger, it will cause pressure changes, in order to simulate the details of the flow field of the cross-flow fan under real working conditions, the simulation assumes that the heat exchanger is a porous medium, and numerical simulation studies are carried out on the cross-flow fan using the porous medium model. The pressure drop of the heat exchanger can be measured through the experiment, then the relationship between velocity and pressure drop can be expressed as:

$$\Delta P = \alpha U^{\beta} \tag{11}$$

where α and β are experimental fitting parameters.

In FLUENT, the momentum source term of the porous medium model can be written as:

$$S_i = -C_0 \mid v \mid^{C_1} \tag{12}$$

where C_0 and C_1 are the fitted empirical coefficients, then $C_0 = \alpha / d$, $C_1 = \beta$, and d is the heat exchanger thickness.

In order to verify the accuracy of assuming the heat exchanger as a porous medium in FLUENT, numerical experiments are needed to validate the porous medium model. The structure of the porous media model is shown in Fig. 1, where a pipe is simulated by CFD and the inlet is set to be the mass flow inlet and the outlet to be the pressure outlet, and a porous media model with the same thickness as the real heat exchanger is placed in the pipe. The results obtained from the test fitting equations and simulations are more consistent, and the use of porous media can realistically simulate the effect of airflow through the heat exchanger on the downstream cross-flow fan.

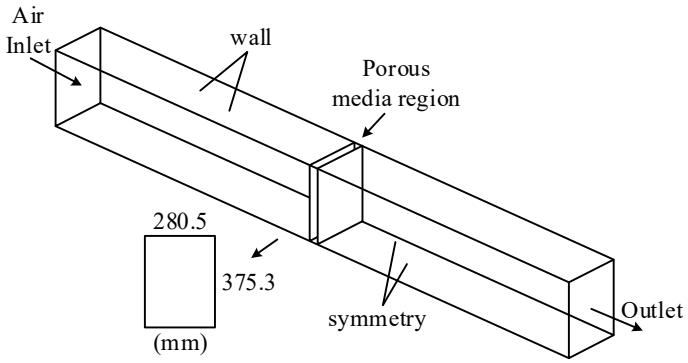

Figure 1: Model of heat exchanger

II. B.Turbulence modeling

In this paper, the fluid inside the plate heat exchanger is in a turbulent state, so a turbulence model needs to be included in the analytical model.

Simcenter STAR-CCM+ is a fluid dynamics (CFD) simulation software used to model phenomena such as fluid flow and heat transfer. The four common types of turbulence models in Simcenter STAR-CCM+ include:

$k-$ model (k-epsilon model): this is one of the most commonly used RANS turbulence models. It is based on two parameters, the turbulent kinetic energy (k) and the turbulent dissipation rate ε, which are used to describe the energy transport and dissipation of turbulence. The $k-\varepsilon$ model is applicable to a wide range of turbulence problems, but may be constrained at high Reynolds numbers and complex flow problems.

The $k-\omega$ model (k-omega model): this is another common RANS turbulence model, also based on turbulent kinetic energy and turbulent dissipation rates. Unlike the $k-\varepsilon$ model, the $k-\omega$ model uses different equations for turbulent kinetic energy to improve predictions in the boundary layer.

SST $k-\omega$ model: this is a modified $k-\omega$ model known as the Shear Stress Transport (SST) $k-\omega$ model. It combines the advantages of both the $k-\varepsilon$ and $k-\omega$ models to improve the overall prediction by using better boundary layer predictions.

Reynolds Stress Model (RSM): This is a more complex RANS turbulence model that takes into account the turbulent stresses in the flow field in all directions.RSM is suitable for more complex flow situations, but also requires more computational resources.

In selecting a suitable turbulence model, factors such as the physical properties involved in the model, simulation objectives and accuracy need to be considered, as well as computational resources and time constraints. Different models are suitable for different flow situations and need to be selected on a problem-specific basis.K-Epsilon models are able to balance factors such as stability, computational cost, and accuracy in a wide range of industrial applications, and are particularly suitable for situations involving complex recirculation, with or without heat transfer. This is due to the relative simplicity and computational efficiency of the K-Epsilon model, which is often required for stability and efficiency in these types of industrial applications.The K-Omega model is similar to the K-Epsilon model in solving the transport equations, with the exception of differences in the choice of the second transport turbulence variable. It is applicable to analytical environments that would typically fall within the range of applicability of the K-Epsilon model.The K-Omega model may provide more accurate results in certain flow situations because it models the flow characteristics in the boundary layer better. The Reynolds stress transport model, on the other hand, is one of the most complex and computationally expensive RANS models, which takes into account turbulent stresses in different directions in the flow field and is suitable for turbulent situations with strong anisotropy. This type of model is recommended only for problems that require more accurate simulation of turbulence characteristics and turbulence anisotropy, such as in equipment with strongly turbulent flow such as cyclone separators.

Therefore, the K-Epsilon turbulence model is chosen in this paper.

The K-Epsilon turbulence model contains two main transport equations, the transport equations are the turbulent kinetic energy K equation (13) and the kinetic energy dissipation rate ε equation (14):

K equation:

$$\frac{\partial(\rho k)}{\partial t}+\nabla\cdot(\rho k\vec{v})=\nabla\cdot\left[\left(\mu+\frac{\mu_t}{\sigma_k}\right)\nabla k\right]+P_k-\rho(\varepsilon-\varepsilon_0)+S_k \tag{13}$$

ε Equation:

$$\frac{\partial(\rho\varepsilon)}{\partial t}+\nabla\cdot(\rho\varepsilon\vec{v})=\nabla\cdot\left[\left(\mu+\frac{\mu_t}{\sigma_\varepsilon}\right)\nabla\varepsilon\right]+\frac{1}{T_e}C_{\varepsilon1}P_\varepsilon-C_{\varepsilon2}f_2\rho\left(\frac{\varepsilon}{T_e}-\frac{\varepsilon_0}{T_0}\right)+S_\varepsilon \tag{14}$$

where $\vec{v}$ is the mean velocity, μ is the dynamical viscosity, σ_k, σ_ε and $C_{\varepsilon1}$ and $C_{\varepsilon2}$ are the model coefficients, and P_k and P_ε are the outcome terms. f_2 is the damping function, S_k and S_ε are user-specified source terms, and ε_0 is the value of ambient turbulence in the source term that counteracts turbulence attenuation.

The K-Epsilon model contains six variants, and the realizable K-Epsilon two-layer model is chosen based on the characteristics of the model in this paper.

II. C. Optimization design ideas and methods

The goal of heat exchanger heat transfer performance optimization design is to meet the process requirements under the premise of reasonable choice of heat exchanger structural parameters and operating parameters, maximize the heat transfer coefficient, reduce the pressure drop, so as to improve the heat transfer efficiency of the heat exchanger as a whole. Optimization of the design needs to take into account the thermal calculation, fluid mechanics analysis, strength calibration and other factors, while taking into account the equipment investment costs and operating costs. The basic idea of optimal design is to fully understand the heat transfer mechanism of the heat exchanger on the basis of mathematical models and optimization algorithms, the impact of the heat transfer performance of the key parameters of the preferred and combined to obtain the optimal design.

Commonly used optimization design methods include parameter optimization method, shape optimization method and topology optimization method. Parameter optimization method is to improve the performance of heat exchanger by optimizing the parameters such as tube diameter, tube length, tube arrangement, etc. under a given heat exchanger structure form. Shape optimization method is to keep the topology of the heat exchanger unchanged, optimize the heat exchanger flow path shape, such as the use of spiral tube, bellows and other enhanced heat transfer elements. Topology optimization method is in a given design space, through the optimization of material distribution, to find the optimal heat exchanger structure layout.

In actual design, numerical simulation is often used in combination with optimization algorithms. Using numerical simulation tools such as computational fluid dynamics, the flow heat transfer process inside the heat exchanger can be finely simulated to obtain detailed information such as velocity field, temperature field, etc., so as to provide a basis for the optimization design. Meanwhile, heuristic optimization algorithms such as genetic algorithm and particle swarm algorithm can be used to search the design space efficiently and find the optimal design point. The iteration of numerical simulation and optimization algorithms can continuously improve the design scheme, and finally obtain the optimal design that meets the requirements.

III. Fluid Dynamics Simulation for Heat Transfer Performance Optimization of Air Conditioning Heat Exchangers

An existing conventional shell-and-tube air conditioning heat exchanger was selected as the experimental object. The specific parameters of the heat exchanger were heat transfer area of 150 m, shell diameter of 1.36 m, and length of 3.15 m. The heat exchanger tubes were conventional smooth tubes, with an outer diameter of 30 mm, a wall thickness of 3.2 mm, and a tube length of 1.8 m. A total of 1,350 tubes were used. The spacing of the folding plate is 0.42 m. The key performance parameters such as heat transfer efficiency, energy consumption and floor space are recorded. This paper mainly explores the influence of different geometrical parameters on the flow heat transfer performance of the air conditioning heat exchanger through numerical simulation, and proposes the corresponding optimized design based on the influence effect.

III. A. Grid independence and computational model validation

III. A. 1) Verification of lattice independence

In this paper, ICEM CFD is used for meshing the fluid domain. In order to save computational time and memory resources, a hexahedral mesh is used in the core fluid domain, thus reducing the total number of meshes while improving the mesh quality. The transition between the prismatic layer mesh near the wall and the hexahedral mesh in the core is made with the help of a pyramidal pentahedral mesh. The number and quality of meshes directly affect the calculation speed and accuracy of the numerical simulation. In general, the finer and more numerous the

meshing, the higher the accuracy of the numerical simulation calculations, and the time required for the calculations may also be longer. In order to save computation time and memory resources under the premise of ensuring the accuracy of simulation results, the grid independence verification should be carried out firstly before formally starting the simulation calculation. In this paper, three different grid sizes are used to generate three grid systems from sparse to dense for the model with the same geometrical parameters, and the numerical simulations under the working condition of Re=4899 are carried out respectively. The results of grid independence verification are shown in Table 1. It can be seen that the relative deviation of Nusselt number is only 0.475% for grid number 12864431 and 28478534, and the relative deviation of flow friction resistance coefficient is only 1.26%, which is not more than 1.5%, which indicates that the grid system of the partitioning strategy 2 can satisfy the requirement of the accuracy of the calculations, and therefore, this paper selects the partitioning strategy 2 as the subsequent numerical simulation grid partitioning work. This indicates that the meshing system of strategy 2 can meet the accuracy requirements of calculation, so this paper chooses the meshing strategy 2 as the subsequent numerical simulation meshing.

Table 1: Results of grid independence verification

Division strategy	The number of grids	Nu	err,%	f	err,%
1	8028671	138.48	5.98	0.1037	1.94
2	12864431	148.96	0.475	0.0971	1.26
3	28478534	149.23	/	0.0962	/

III. A. 2) Computational model validation

Numerical simulation is to simulate the actual experimental or engineering situation through iterative calculations, so it is necessary to use appropriate calculation models and settings, and then compare the obtained results with experimental data or empirical formulas in order to prove the feasibility and accuracy of the numerical simulation scheme. Based on the verification of grid independence, this paper uses the same meshing strategy to model and mesh a smooth casing shell course of the same size to carry out numerical simulations, and the comparison of the computational results with the empirical formulas is shown in Fig. 2. The maximum relative deviation of the Nusselt number is 1.93%, and the maximum relative deviation of the friction resistance factor is 3.67%, which are both less than 5%, proving that the turbulence model adopted in this paper can accurately predict the flow and heat transfer characteristics of the casing shell course, and the boundary conditions and settings in the numerical simulation are also reliable.

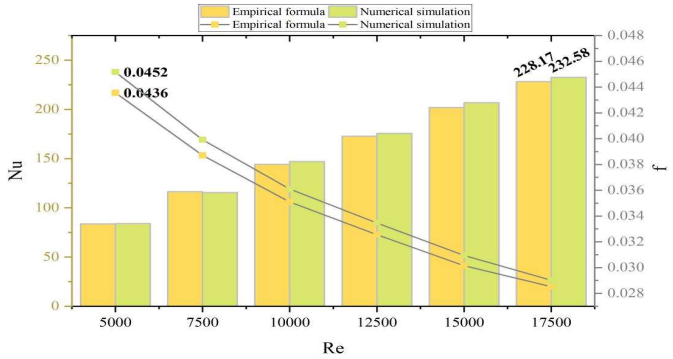

Figure 2: Comparison of the calculated results with the empirical formula

III. B. Analysis of the effect of geometrical parameters on flow heat transfer performance

III. B. 1) Effect of pitch on flow heat transfer performance

In this section, the effect of discontinuous diagonal rib axial upward pitch (adjacent spacing) on the performance of air-conditioning heat exchangers is investigated by selecting a discontinuous diagonal rib casing with inclination angle $\theta = 30°$, circumferential number $n = 6$, and using the control variable method by varying only the diagonal rib pitch $S = 2.5/3.75/5\text{mm}$ using smooth casing under the same flow conditions and numerical simulation settings, and the results are compared and analyzed. The trends of Nusselt number growth factor, friction resistance coefficient growth factor and comprehensive performance index PEC with Reynolds number for different pitch parameters relative to the smooth casing are shown in Fig. 3, where the Nusselt number growth factor indicates the multiplier of heat transfer capacity enhancement. The heat transfer capacity of discontinuous diagonal rib casing is

obviously stronger than that of smooth casing, especially in low Reynolds number condition, the effect of enhanced heat transfer is more obvious, and the Nusselt number can reach 2.18 times of the smooth casing at most. The flow resistance of the casing shell course is also increased by the discontinuous diagonal ribs, and the maximum f / f_0 is 3.41.

The trends of Nu / Nu_0 and f / f_0 with pitch of diagonal ribs are approximately the same, which is more in line with the expectation that the smaller the pitch between diagonal ribs, the denser they are arranged in the axial direction, the stronger the perturbation effect on the fluid, and the stronger the effect of enhanced heat transfer, and correspondingly, more increase in the pressure drop in the shell course. It is worth noting that the trends of Nu / Nu_0 and f / f_0 with the Reynolds number are completely opposite, with the increase of the Reynolds number, the effect of the enhanced heat transfer is weakened, while the shell flow resistance increases significantly, indicating that the discontinuous diagonal-ribbed casing has a better performance in turbulent flow conditions at low Reynolds numbers. The variation of Nu / Nu_0 and f / f_0 over the range of geometrical parameters and Reynolds numbers studied are 1.65-2.18 and 1.98-3.41, respectively.

The PECs corresponding to all the studied geometric parameters and Reynolds numbers are greater than 1, proving that the discontinuous diagonally ribbed casing has good overall performance. It is not difficult to find that the variation of PEC shows a decreasing trend with the increase of Reynolds number, which is due to the fact that Nu / Nu_0 and f / f_0 decrease and increase with the increase of Reynolds number, respectively, and so the comprehensive performance shows a decreasing trend. Besides, at the same Reynolds number, the PEC increases with decreasing the pitch of the diagonal ribs, which indicates that although decreasing the pitch increases both Nu / Nu_0 and f / f_0 , the ratio of the two also increases the PEC obtained, which shows that the heat transfer enhancement gained from decreasing the pitch of the discontinuous diagonal ribs outweighs the cost of the increase in flow resistance. It is worth mentioning that, from the results, if the pitch is further reduced, perhaps there is still room to improve the PEC, but considering the number of meshes and the difficulty of actual production and processing, this paper does not do the study of discontinuous diagonal rib casing with a pitch less than 2.5 mm, so $S = 2.5mm$ is chosen as one of the optimized structural parameters. In the range of geometric parameters and Reynolds number studied, the PEC varies from 1.19 to 1.64.

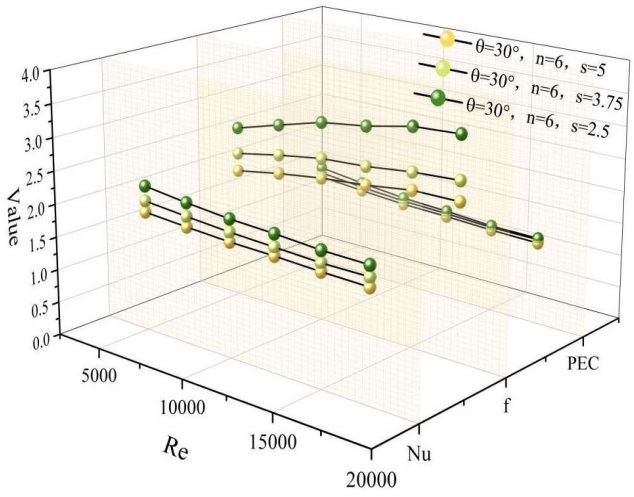

Figure 3: The influence of pitch on the flow heat transfer performance

III. B. 2) Effect of tilt angle on flow heat transfer performance

In this paper, we investigate the effect of the inclination angle of discontinuous diagonal ribs on the performance of air-conditioning heat exchangers. Discontinuous diagonal rib casing with pitch $S = 2.5mm$ and circumferential number $n = 6$ was selected, and the results were compared and analyzed by using the control variable method, varying the inclination angle only $\theta = 30° / 40° / 50° / 60°$, also using smooth casing under the same flow conditions and numerical simulation settings, the results are compared and analyzed. The trends of Nusselt number growth factor, flow friction resistance factor growth factor and overall performance index PEC with Reynolds number for discontinuous diagonally ribbed casing relative to smooth casing at different inclination angle parameters are shown in Fig. 4. Even if the inclination angle is different, the trend of Nu / Nuu_0 with Reynolds number is always the same,

and all of them decrease with the increase of Reynolds number, which proves again that discontinuous diagonal-ribbed casing is more capable of reinforcing the heat transfer under the low Reynolds number working condition. In addition, the larger the inclination angle, the more heat transfer capability is enhanced, which is due to the stronger disturbing effect of the inclined rib with larger inclination angle, and the maximum Nusselt number is 2.55 times that of the smooth casing. Correspondingly, the flow resistance of the casing shell course also increases significantly with the increase of the inclination angle of the diagonal ribs, and the maximum f/f_0 is 5.90 at the inclination angle of $60°$. The overall rule of change is more in line with expectations, but it is worth noting that when the tilt angle is increased from $50°$ to $60°$, the increase ratio of Nusselt number is only very small, while the increase ratio of friction resistance factor is still increased significantly, indicating that the cost of flow resistance is still increased after the tilt angle is increased to a certain extent, and the gain for heat transfer capacity enhancement will become very limited. For the studied range of geometrical parameters and Reynolds number, Nu/Nu_0 and f/f_0 are varied in the range of 1.98-2.55 and 2.65-5.90, respectively.

The PEC corresponding to all tilt angles and Reynolds numbers studied are greater than 1, proving that the performance is better at different tilt angles. It is not difficult to find that the larger the tilt angle is, the steeper the curve of PEC with Reynolds number is, and the curve of $\theta = 60°$ is especially obvious, while the curves of $\theta = 30°$ and $\theta = 40°$ are very close to each other and nearly overlap. Besides, the PEC of inclined angles $50°$ and $60°$ are relatively high at low Reynolds numbers, but relatively low at Reynolds numbers higher than 7305, indicating that inclined ribs with larger inclined angles are more suitable for application at low Reynolds number conditions. The PEC varies from 1.30 to 1.58 over the range of tilt angles and Reynolds numbers studied. In a comprehensive comparison, $30°$ and $40°$ inclined angle of discontinuous inclined rib casing have better overall performance, considering the better enhanced heat transfer effect under $40°$ inclined angle, so $\theta = 40°$ is selected as one of the optimized structural parameters in this paper.

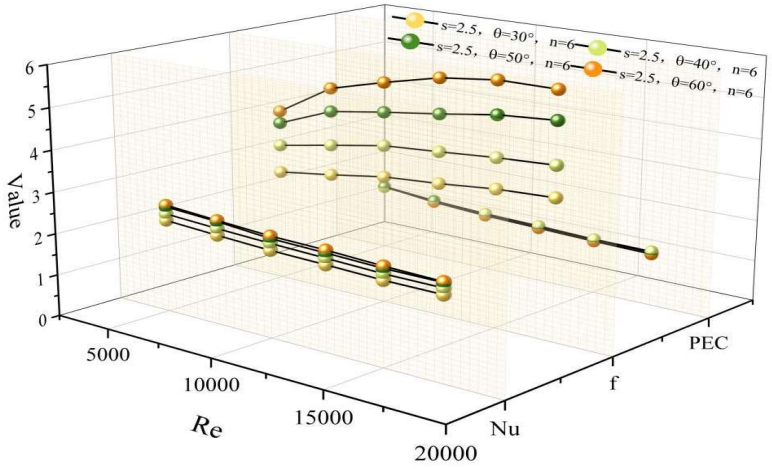

Figure 4: The influence of tilt Angle on the flow heat transfer performance

III. C. Analysis of experimental results

III. C. 1) Comparison of heat transfer efficiency

The optimized air conditioner heat exchanger shows significant improvement in heat transfer efficiency. The air conditioner heat exchanger before and after optimization was subjected to 800 simulation experiments to compare the heat transfer efficiency of the two air conditioner heat exchangers, and the comparison results are shown in Figure 5. Before the optimization of the air conditioner heat exchanger, its heat transfer efficiency was 3500W/(m2·K) on average, while after the optimization, the heat transfer efficiency of the air conditioner heat exchanger increased to 3850W(m2·K), which is an average increase of 350W/(m2·K). Specific data show that, compared with the original design, the optimized air-conditioning heat exchanger heat transfer efficiency has increased by about 10 per cent, and the exchange of heat between hot and cold fluids is more efficient.

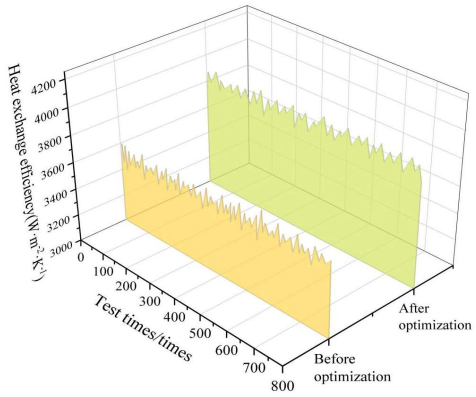

Figure 5: Comparison of heat transfer efficiency before and after optimization

III. C. 2) Changes in energy consumption and pressure drop

In terms of energy consumption, the optimized air conditioning heat exchanger also shows obvious advantages. The energy consumption and pressure drop of the air-conditioning heat exchanger before and after optimization and its footprint are compared, and the results of each index are shown in Table 2. The energy consumption of the air conditioning heat exchanger before optimization is 147kW, and after optimization, the energy consumption of the air conditioning heat exchanger is reduced to 129kW. In addition to the improvement of heat transfer efficiency and energy consumption, the optimized air conditioning heat exchanger also shows obvious advantages in terms of structural compactness and ease of maintenance, and the floor space has been reduced by about 52m, which is more adaptable to the needs of the compact layout of modern industrial production. At the same time, the maintenance of the air conditioning heat exchanger is more convenient, and the service life has been extended, and the maintainability has been increased by 26%. In summary, the experimental results fully prove the effectiveness of the proposed optimized design method of the air conditioning heat exchanger. The optimized air conditioning heat exchanger shows significant improvement in heat transfer efficiency, energy consumption, compactness and ease of maintenance, which provides strong support for the progress and development of industrial production.

Table 2: Results of changes in various indicators

	Before optimization	After optimization
Energy consumption/kW	147	129
Land area/m^2	258	206
Service life/years	12	25
Maintainability/%	57	83

Table 3: Comparison results of each parameter

Flow path form	Original plan	Optimization plan 1	Optimization plan 2	The proposed
Total heat exchange capacity/W	1497.28	1511.35	1562.47	1593.28
Latent heat/W	297.21	300.27	317.38	342.56
Latent heat proportion/%	19.77	20.99	21.33	21.85
Dehumidification capacity/(g/h)	442.18	459.37	478.26	492.15
Pressure drop inside the pipe/kPa	4.27	4.27	4.29	4.27

III. C. 3) Comparative analysis of programs

Different optimization schemes are used for simulation calculation, and the comparison results of each parameter are shown in Table 3. The different optimization schemes have almost no effect on the pressure drop in the tube, and the four parameters of total heat transfer, latent heat, latent heat percentage and dehumidification capacity of the air conditioning heat exchanger under the optimization scheme of this paper are the largest, followed by the air conditioning heat exchanger of the control scheme 1, and the air conditioning heat exchanger of the control scheme 2 is the smallest. Compared with the prototype, the optimized solution in this paper improves the total heat transfer capacity by 6.41%, the latent heat capacity by 15.26%, the latent heat percentage by 10.52%, and the dehumidification capacity by 11.30%. It shows that the optimized design in this paper can enhance the heat

exchange as well as increase the dehumidification efficiency of the air conditioning heat exchanger, i.e., the optimized design is effective.

IV. Conclusion

In this paper, based on the fluid dynamics simulation, the numerical simulation of the air conditioner heat exchanger is carried out, and the corresponding optimization strategy is proposed and its effectiveness is investigated.

The relative deviation of Nusselt number is only 0.475% for grid number 12864431 and 28478534, while the relative deviation of flow friction resistance factor is only 1.26%, which is not more than 1.5%. Therefore, we choose mesh division strategy 2 for numerical simulation mesh division. The maximum relative deviation of the Nusselt number is 1.93% and the maximum relative deviation of the friction resistance factor is 3.67%, which are both less than 5%, proving that the turbulence model adopted in this paper can accurately predict the flow and heat transfer characteristics of the casing shell course.

The angle of inclination $\theta = 30°$, the number of circumferences $n = 6$, the pitch $S = 2.5/3.75/5\text{mm}$, and the ranges of variation of Nu/Nu_0 and f/f_0 are 1.65-2.18 and 1.98-3.41, respectively, and the variation of PEC range is 1.19-1.64.The pitch $S = 2.5\text{mm}$, the number of circumferences $n = 6$, the angle of inclination $\theta = 30°/40°/50°/60°$, Nu/Nu_0 and f/f_0 are varied in the range of 1.98-2.55 and 2.65-5.90, respectively, and the PEC is varied in the range of 1.30-1.58. $S = 2.5mm$ and $\theta = 40°$ are chosen as the optimized structural parameters.

The heat transfer efficiency of the optimized air-conditioning heat exchanger has increased to 3,850 W (m2·K), an average increase of 350 W/(m2·K), an increase of about 10% in heat transfer efficiency, and a more efficient exchange of heat between hot and cold fluids. In terms of energy consumption, the optimized air conditioning heat exchanger also shows obvious advantages. The energy consumption of the optimized air conditioning heat exchanger is reduced to 129kW, the footprint is reduced by about 52m, and the maintainability is increased by 26%. Using different optimization schemes for simulation calculation, the total heat transfer, latent heat, latent heat percentage and dehumidification of the air conditioning heat exchanger under the optimization scheme of this paper have the largest four parameters, with the total heat transfer increased by 6.41%, latent heat increased by 15.26%, latent heat percentage increased by 10.52%, and dehumidification increased by 11.30%. It shows that the optimized design of this paper can strengthen the efficiency of heat transfer and dehumidification, and realize the optimization of heat transfer performance of air conditioner heat exchanger.

References

[1] Yang, L., Yan, H., & Lam, J. C. (2014). Thermal comfort and building energy consumption implications–a review. Applied energy, 115, 164-173.

[2] Yang, Z., Du, C., Xiao, H., Li, B., Shi, W., & Wang, B. (2022). A novel integrated index for simultaneous evaluation of the thermal comfort and energy efficiency of air-conditioning systems. Journal of Building Engineering, 57, 104885.

[3] Yan, H., Pan, Y., Dong, M., Zhang, H., Li, J., & Zhao, S. (2025). Energy efficiency and comfort: analysis of thermal responses and behaviors of residents with high and low air conditioning dependency. Energy and Buildings, 115695.

[4] Lim, D. K., Ahn, B. H., & Jeong, J. H. (2018). Method to control an air conditioner by directly measuring the relative humidity of indoor air to improve the comfort and energy efficiency. Applied energy, 215, 290-299.

[5] Hernández, F. F., Suárez, J. M. P., Cantalejo, J. A. B., & Muriano, M. C. G. (2022). Impact of zoning heating and air conditioning control systems in users comfort and energy efficiency in residential buildings. Energy Conversion and Management, 267, 115954.

[6] Li, Q., Zhou, Y., Wei, F., Long, Z., Li, J., Ma, Y., ... & Yu, D. (2024). Harmonizing comfort and energy: A multi-objective framework for central air conditioning systems. Energy Conversion and Management, 314, 118651.

[7] Yang, Z., Dong, X., Xiao, H., Sun, H., Wang, B., Shi, W., & Li, X. (2022). Investigation of thermal comfort of room air conditioner during heating season. Building and Environment, 207, 108544.

[8] Greco, A., & Masselli, C. (2020). The optimization of the thermal performances of an earth to air heat exchanger for an air conditioning system: A numerical study. Energies, 13(23), 6414.

[9] Lim, H., Han, U., & Lee, H. (2020). Design optimization of bare tube heat exchanger for the application to mobile air conditioning systems. Applied Thermal Engineering, 165, 114609.

[10] Tan, L., & Yuan, Y. (2022). Computational fluid dynamics simulation and performance optimization of an electrical vehicle Air-conditioning system. Alexandria Engineering Journal, 61(1), 315-328.

[11] Liu, W., Jin, M., Chen, C., & Chen, Q. (2016). Optimization of air supply location, size, and parameters in enclosed environments using a computational fluid dynamics-based adjoint method. Journal of Building Performance Simulation, 9(2), 149-161.

[12] Roh, J., Kim, Y., & Ahn, J. (2025). Computational-Fluid-Dynamics-Based Optimization of Wavy-Slit Fin Geometry in Indoor Units of Air Conditioners Using Low-Global-Warming-Potential Refrigerants. Applied Sciences (2076-3417), 15(3).

[13] Bacellar, D. (2015). Novel Heat Exchanger Design Using Computational Fluid Dynamics and Approximation Assisted Optimization. ASHRAE Transactions, 121, 1NN.

[14] He, J. (2022, December). Design and Optimization of Automotive Air Conditioning Duct Based on CFD Algorithm. In Journal of Physics: Conference Series (Vol. 2386, No. 1, p. 012095). IOP Publishing.